JOURNAL OF SCIENCE
SAKARYA UNIVERSITY

Sakarya University Journal of Science

ISSN 1301-4048 | e-ISSN 2147-835X | Period Bimonthly | Founded: 1997 | Publisher Sakarya University | http://www.saujs.sakarya.edu.tr/en/

Title: Optimization of Back-Surface Field for Crystalline Silicon Solar Cells and Estimating the Firing Temperature depending on the Amount of Printed Aluminum

Authors: İmran KANMAZ, Abdullah ÜZÜM
Recieved: 2019-11-25 16:47:11

Accepted: 2020-04-26 16:33:52

Article Type: Research Article
Volume: 24
Issue: 4
Month: August
Year: 2020
Pages: 605-614

How to cite
İmran KANMAZ, Abdullah ÜZÜM; (2020), Optimization of Back-Surface Field for Crystalline Silicon Solar Cells and Estimating the Firing Temperature depending on the Amount of Printed Aluminum. Sakarya University Journal of Science, 24(4), 605-614, DOI: https://doi.org/10.16984/saufenbilder.650790
Access link
http://www.saujs.sakarya.edu.tr/en/pub/issue/55932/650790

Sakarya University Journal of Science 24(4), 605-614, 2020

Optimization of Back-Surface Field for Crystalline Silicon Solar Cells and Estimating the Firing Temperature depending on the Amount of Printed Aluminum

İmran KANMAZ*[1], Abdullah ÜZÜM[1,2]

Abstract

Optimization of back surface field (BSF) for crystalline silicon solar cells was carried out by Afors-Het simulation software. Thickness and doping concentration parameters were optimized and electrical parameters of solar cells both with BSF and non-BSF were analyzed. The optimum BSF thickness and doping concentration for the crystalline silicon solar cell were determined as 7 µm and $1x10^{19}$ cm^{-3}, respectively. A special attention was given to the estimation of peak firing temperature considering the printing amount of aluminum paste in order to form an optimal BSF by the calculations using Al-Si binary phase diagram. It was concluded that the temperature of up to 950ºC should be established if an amount of 3 mg/cm^2 printed aluminum was used to achieve BSF thickness of 7 µm, where 775 ºC would be enough when the amount of aluminum is 8 mg/cm^2.

Keywords: Afors-Het, back surface field, fire through, silicon solar cell

1. INTRODUCTION

Crystalline silicon (c-Si) solar cells are most widely used type of solar cell in photovoltaic applications. Reducing the losses in solar cells plays a key role to improve conversion efficiency. Mainly, losses including the reflection of incoming light to the front surface, shading losses of the front contact, resistance losses of metal contacts, and recombination losses of minority carriers in the surface regions with cell structure are the main obstacles [1]. Among them, surface recombination of minority carriers occurs at the back surface of the silicon solar cells is one of the facts which is needed to be considered in cell design. Conventional c-Si solar cells mostly have a fully-screen printed aluminum (Al) on back surface which possesses a high surface recombination velocity if not a highly doped p^+ region is created on the rear surface of the solar cell to minimize the recombination [2]. For instance, a study of back surface field (BSF) formed by the screen-printed and sputtering methods for c-Si solar cells with thermally

*Corresponding Author: imrankanmaz@ktu.edu.tr
[1]Karadeniz Technical University, Department of Renewable Energy Resources/Technologies, Trabzon, Turkey. ORCID: https://orcid.org/0000-0001-8827-1590; https://orcid.org/0000-0001-5324-8892
[2]Karadeniz Technical University, Department of Electrical and Electronics Engineering, Trabzon, Turkey. ORCID: https://orcid.org/0000-0001-5324-8892. E-mail:auzum@ktu.edu.tr

annealing at 700°C to 1000°C, a relative increase of 6% was achieved in efficiency that summarizes the importance of BSF [3]. There are several chief parameters influences the back-side metallization process and BSF including the thickness of BSF, doping concentration of BSF, amount of printed Al paste and firing temperature. The printing amount of Al commercially varies between 3-9 mg/cm^2 which effects other properties of BSF along with the firing temperature. For instance, Al-BSF lay down for a 6-inch industrial solar cell was reported averagely at around 5.4 mg/cm^2 [4]. The importance of the properties of BSF regions was highlighted on recent studies for PERC (Passivated Emitter Rear Contact) solar cells that shows the need of optimization for better local BSF properties [5]. Firing process of Al leading to variation of concentration and the thickness of the layer is a key factor in that sense. Moreover, controlling the concentration of Al doped layers is also crucial for bifacial cell structures where they are utilized as front surface field [6]. Therefore, optimization of the printing amount of Al and the firing temperature and understanding their effects on the other parameters of BSF are important to have a quality BSF layer.

On the other hand, it is well-known that simulation and calculations can be supportive to canalize the experimental studies. Several solar simulation programs including PC1D, Opal, Afors-Het, Silvaco atlas and Matlab software are used for the simulation of solar cells where some of them free of charge and some of them costly. Afors-Het is a one-dimensional numerical computer software used for modeling multilayer homo or heterojunction solar cells and some common methods for characterization of solar cells [7]. M. Schmidt *et al.* investigated the basic properties of amorphous/crystalline heterojunction (a-Si:H/c-Si), and their effect on recombination of excess carriers. Using the surface photovoltage analysis and Afors-Het simulation software, they achieved an optimal doping for an efficient a-SiH/c-Si solar cell without an i-type a-Si:H buffer layer and a efficiency of 19.8% for the coating temperature of 210°C [8]. In another study, different parameters of heterostructure thin films were optimized with Afors-Het to show that a high performance of up to 25% efficiency can be achieved by using nanostructured surfaces for HIT silicon solar cells [9]. Neeraj Dwivedi *et al.* optimized the thicknesses of n-type a-Si:H emitter layer, front a-Si:H i-layer and p-type c-Si base as well as optimum heterojunction (HJ) and HJ with intrinsic layer (HIT) solar cells using Afors-Het and reported an efficiency of 27.02% in the bifacial HIT solar cell. Optimized thicknesses of n-type a-Si:H emitter layer and front a-Si:H i-layer were introduced as 6 nm and 3 nm respectively with 200 μm base substrate thicknesses of c-Si [10]. Afors-Het is generally used in the simulation of heterojunction solar cells effectively and not much for conventional c-Si solar cells.

In this study, optimization of BSF layer for c-Si solar cells was carried out by Afors-Het software in order to determine the optimum thickness and doping concentration of the BSF [7]. A special attention was given to the optimization of the printing amount of Al paste and the related firing temperature according to the binary phase diagram of Al-Si to achieve the optimized BSF parameters obtained by Afors-Het simulations. The role of BSF phenomenon and the correlation of the facts from processing to the design was also discussed and analyzed for better understanding of BSF structure.

2. METHODS

In this section, the structure of a BSF and its effect on the performance of a solar cell were explained. Typical firing profile for Al fire through process given with related calculations. Initial parameters for simulation and the simulation flow were also explained.

2.1. Back Surface Field (BSF) Structure

Minimizing surface recombination losses is crucial for the development of a high efficiency solar cells [11]. The presence of a potential barrier on the back of a conventional silicon solar cell can significantly improve the performance of the cell by increasing mainly the open circuit voltage *(V_{OC})* and short circuit current *(I_{SC})* owing to the minimized recombination. In order to achieve

such effect behind the $n^+/p/p^+$ structure to provide a significant improvement in cell performance, the minority carrier diffusion length in the base region should exceed the base thickness [12].

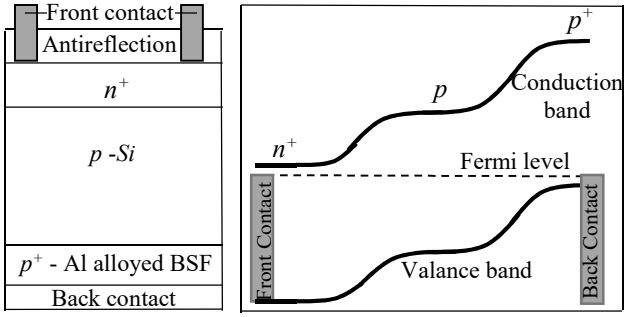

Figure 1. Schematic representations of a typical p-type c-Si solar cell with Al-alloyed BSF (a), Energy band diagram of BSF (b)

The schematic representation of the Al-alloyed BSF and the energy band diagram of the BSF are shown in the Figure 1. With the energy barrier formed between the p/p^+ junction, less of minority charge carriers formed at the base can be recombination on the rear surface. The BSF function acts like a mirror pushing carrier charges back into the cell [2]. Commonly, this effect of backside passivation is performed by alloying a screen-printed Al paste with silicon which establishes a moderate level of the BSF in commercial cell structures.

Effective back surface recombination velocity (SRV) which is a parameter to evaluate the passivation performance, can be in the range of 80-200 cm/s for boron BSF cells, while effective rear SRV of Al-BSF cells were recorded as 260-700 cm/s [13]. A back-surface recombination rate of 200 cm/s can be achieved by printing a thick layer of Al over 20 μm and firing at temperatures above 800°C for 1-5 minutes [11]. However, this process leads to a significant warpage of the wafer, which can lead to a problem with low mechanical yield when using thin substrates [14]. It is important to decrease the amount of Al in such cases which brings the necessity to optimize firing process. Therefore, it is rewarding to estimate the optimal firing temperature and effected parameters depending on the amount of printed Al paste. Furthermore, Ag is used for front contacts and the alloying process of Ag/Si and Al/Si is commonly performed by a co-firing process. During the co-firing process, the wafers undergo a rapid treatment with a certain temperature profile similar to that of in Figure 2. This results in chemical and structural changes inside the printed pastes and substrate surfaces where Al pastes consists of Al particles with various diameter ranges, organic binders, solvents and glass frit [15]. During the firing process, Al-Si alloying takes place according to the Al-Si phase diagram [14]. An example of the temperature profile of a firing process was given in Figure 2, which can be summarized as: Solvents were removed during the drying of the screen-printed Al paste and a surface of silicon substrate with attachment of 50-70% by binders is achieved [16]. Binders burn out by increasing the temperature and alloying process of Al with silicon starts locally at around 660°C by diffusing of silicon through contacted regions. Penetration of Al into the silicon takes place with further increase of temperature and forms local spikes which expands horizontally. In addition to that molten Al-Si area acts as a sink for many contaminants and gives a perfect gettering effect. At peak temperature Al-Si liquid region is established. Al forms a eutectic alloy with silicon at a temperature of 577°C. Epitaxial recrystallization occurs by rejection of silicon during the cooling down and silicon is doped with Al at its solubility limit of Al at a given temperature, thereby producing a p^+- BSF layer [14, 16].

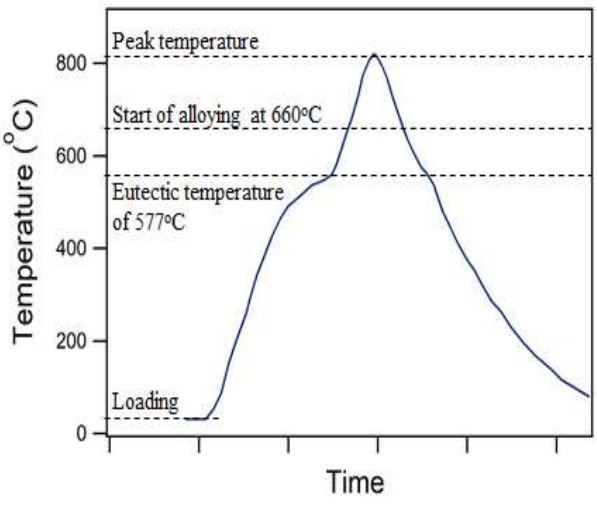

Figure 2. An example of temperature profile for the co-firing process.

Sufficient thickness of Al-BSF layer is necessary to obtain according to the Al-Si binary phase diagram where solubility of the silicon in the Al melt reaches 1.6 wt% at eutectic temperature of 577°C [17]. The concentration of silicon corresponding to the eutectic reaction has been reported in a variety of ranges such as 11.9 wt%, 12.2 wt%, 12.3 wt% and 12.6 wt% [18]. The BSF thickness can theoretically be calculated from the formulation of [3]:

$$W_{BSF} = \frac{m_{Si}}{Ax\rho_{Si}}, \quad (1)$$

$$m_{Si} = m_{Al}\left(\frac{F}{100-F} - \frac{E}{100-E}\right), \quad (2)$$

where m_{Si} is the Si mass dissolved, m_{Al} is the mass of deposited Al, ρ_{si} is the density of the silicon, A is the area of the sample, F and E are the percentage of Si mass in the liquid, at the firing temperature and at the eutectic, respectively [3].

2.2. Simulation

Optimization of the BSF layer which significantly improves the efficiency of c-Si solar cells was carried out using Afors-Het software. The influence of thickness and doping concentration on solar cell performance was specifically considered. Firstly, the effects of BSF thickness on solar cell efficiency was examined. Thickness of BSF was varied from 1 µm to 30 µm while other parameters kept constant. Table 1 shows the fixed values.

Table 1. Some initial parameter values for c-Si solar cell.

Emitter thickness (µm)	0.3
Emitter doping concentration (cm^{-3})	$1x10^{20}$
Reflectance (%)	8
Base Thickness (µm)	200
Base doping concentration (cm^{-3})	$1.5x10^{16}$
BSF doping concentration (cm^{-3})	$1.0x10^{19}$
Series resistance (Ω cm^2)	0.8
Parallel resistance (Ω cm^2)	10000

Secondly, the effect of BSF concentration on efficiency by varying the doping concentration from 1×10^{16} cm^{-3} to 5×10^{20} cm^{-3} was analyzed while keeping the BSF thickness constant at 7 µm.

Electrical characteristics of the cells including J_{SC}, V_{OC}, fill factor *(FF)* and efficiency values were calculated from *I-V* graphs. J_{SC}, V_{OC} and efficiency dependence on doping concentration were discussed separately. At last, theoretical BSF thicknesses depending on the peak firing temperature were calculated using Equation (1) and (2) in order to clarify the required temperatures for optimal BSF thickness.

3. RESULTS AND DISCUSSION

In this section, the results of optimization of the back-surface field parameters according to the simulations were given and discussed. Determining the optimal firing temperature for expected parameters including BSF thickness and the printed Al paste amount were explained as well.

3.1. Optimization of Back Surface Field Layer

Table 2 presents the dependence of the electrical parameters on the BSF thickness. *I-V* characteristics and current density dependence on BSF thickness can be seen in Figure 3. The J_{SC} of the cell increased with increasing BSF thickness from 31.95 mA/cm^2 to 32.11 mA/cm^2.

Table 2. Electrical characteristic dependence on BSF thickness.

BSF Thickness (µm)	Voc (mV)	Jsc (mA/cm^2)	FF (%)	Eff (%)
1	680.5	31.95	80.55	17.51
2	689.6	32.01	80.63	17.80
4	695.3	32.04	80.69	17.98
5	696.2	32.05	80.70	18.01
6	696.6	32.06	80.69	18.02
7	696.7	32.06	80.69	18.02
8	696.6	32.06	80.69	18.02
9	696.4	32.07	80.69	18.02
10	696.1	32.07	80.69	18.01
12	695.3	32.08	80.69	18.00
15	693.9	32.08	80.69	17.96
20	691.3	32.09	80.68	17.90
25	689.0	32.10	80.62	17.83
30	686.8	32.11	80.62	17.78

V_{OC} increased with increasing the BSF thickness and reached maximum value of 696.70 mV at BSF thickness of 7 µm. However, V_{OC} decreased when the BSF thickness was wider than 7 µm. Efficiency increased with increasing BSF thickness and remained constant at 18.02% when the thickness of BSF is between 6 µm and 9 µm where V_{OC} was slightly higher in case the BSF thickness was 7 µm. These results for BSF thickness are quite consistent with experimental data. The experimental value of the BSF thickness was reported as 6.8 µm [3]. In another study, 50% Al coated contacts for best multi crystal and mono crystal cells were obtained local BSF thicknesses of 5 to 7 µm where *FF* values of 78% and 77% [19].

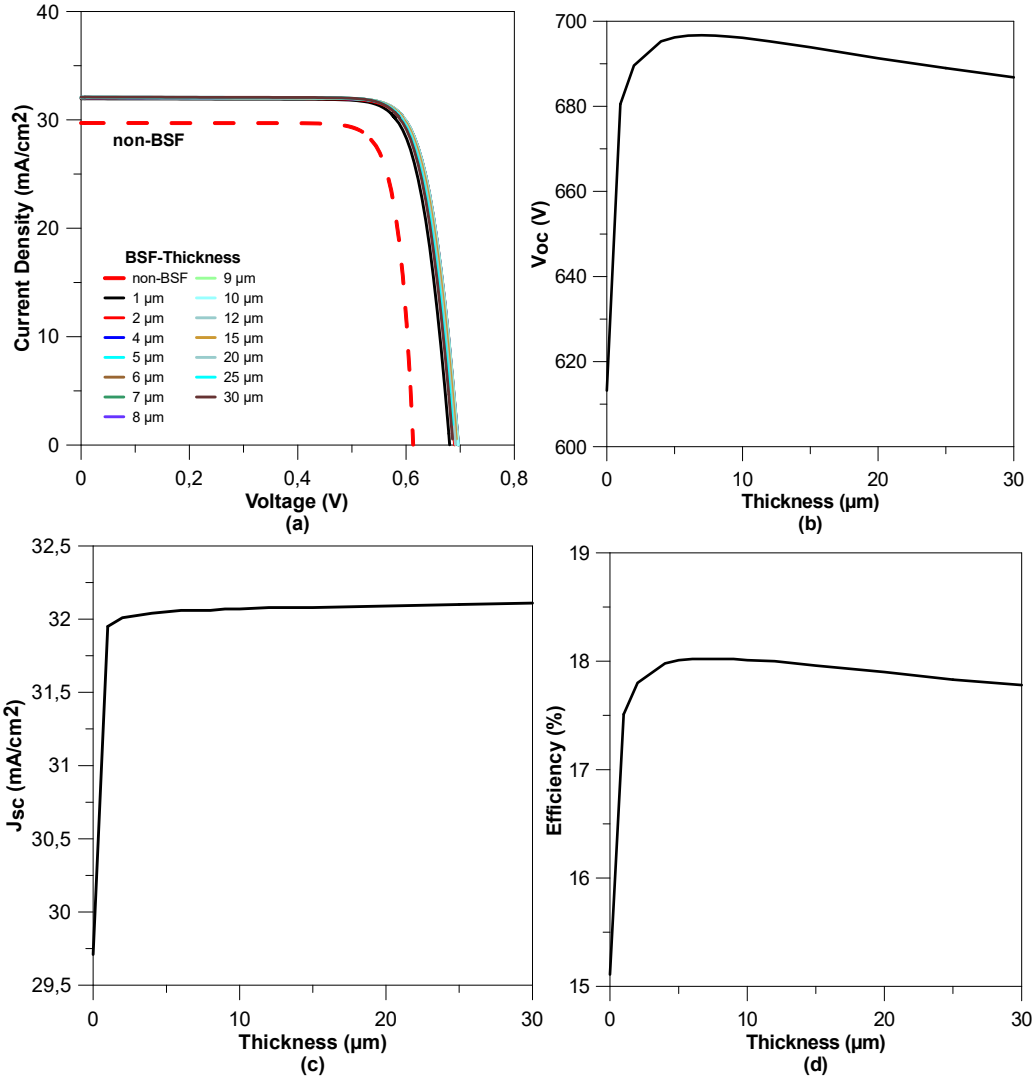

Figure 3. Characteristics of c-Si solar cells depending on BSF thickness

After these optimizations BSF thickness was fixed to 7 µm and doping concentration was varied from 1×10^{16} cm^{-3} to 5×10^{20} cm^{-3} in order to investigate the effect of the BSF doping concentration on the characteristics of the c-Si solar cell.

As shown in Table 3, an increase in V_{OC}, *FF*, and J_{SC} was observed as a result of increasing BSF doping concentration from 1×10^{16} cm^{-3} to 1×10^{19} cm^{-3} for c-Si solar cell. Figure 4 illustrates the electrical characteristics including *I-V* and efficiency, V_{OC} and J_{SC} dependence on the doping concentration of the c-Si solar cell.

Table 3. Cell parameters varying with BSF doping concentration.

BSF Na (cm^{-3})	Voc (mV)	Jsc (mA/cm^2)	FF (%)	Eff (%)
1×10^{16}	613.8	29.76	79.32	14.49
5×10^{16}	616.6	30.00	79.37	14.68
1×10^{17}	620.6	30.29	79.39	14.92
5×10^{17}	644.3	31.39	79.89	16.16
1×10^{18}	659.5	31.73	80.18	16.78
5×10^{18}	689.9	32.03	80.62	17.82
1×10^{19}	696.7	32.06	80.69	18.02
5×10^{19}	685.4	32.06	80.69	17.99
1×10^{20}	688.1	32.02	80.63	17.77
5×10^{20}	661.5	31.76	80.23	16.86

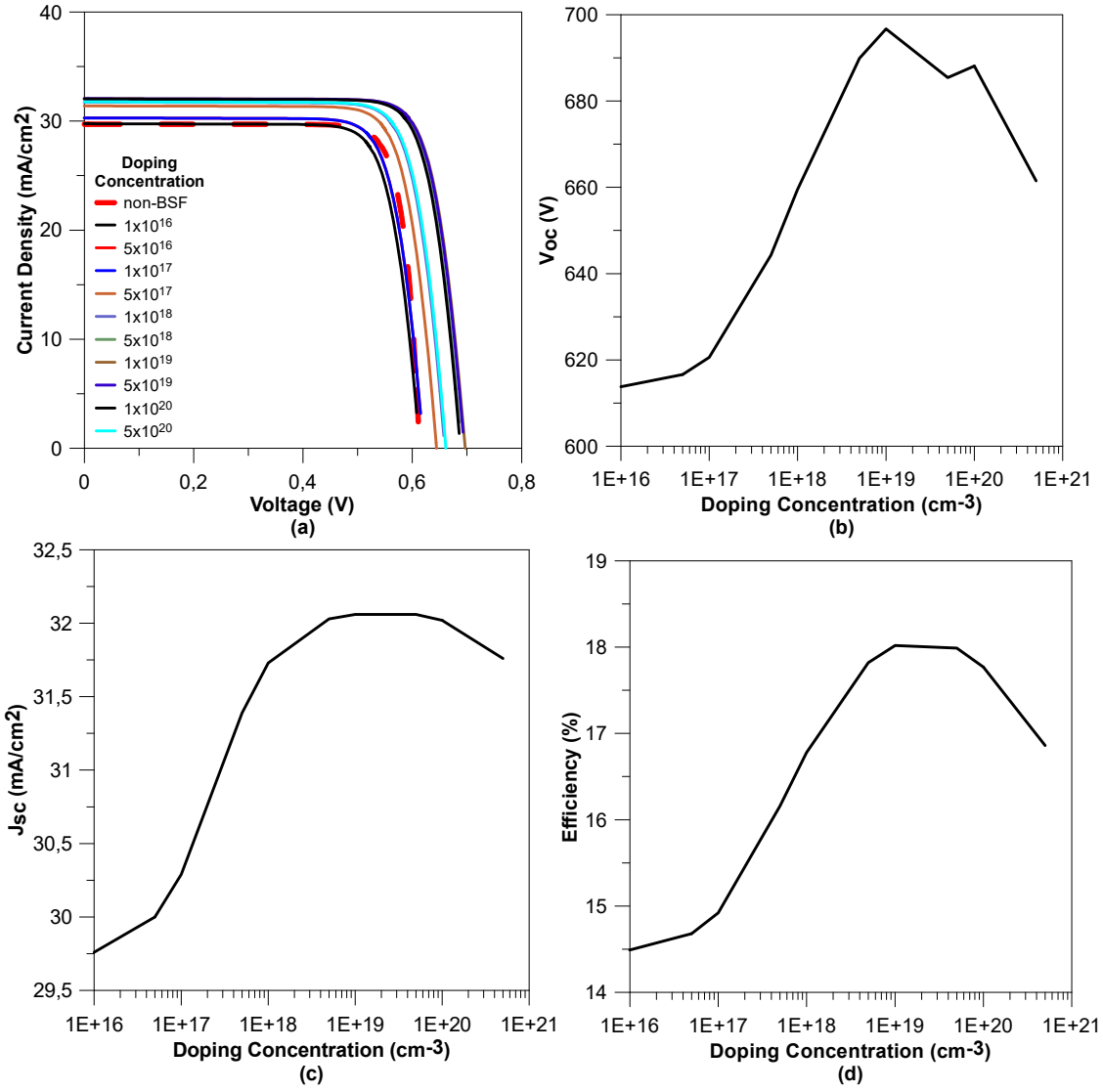

Figure 4. Electrical characteristics of c-Si solar cells depending on BSF doping concentration

The efficiency of the solar cell increased from 14.49% to 18.02%, respectively by increasing doping concentration of BSF from 1×10^{16} cm^{-3} to 1×10^{19} cm^{-3}. However, by increasing the doping concentration from 5×10^{19} cm^{-3} to 5×10^{20} cm^{-3} the efficiency decreased from 18.02% to down to 16.86%. The optimal doping concentration of BSF was 1×10^{19} cm^{-3} with efficiency of 18.02%. The optimum BSF doping concentration has been reported experimentally as around the similar values in 1×10^{19} cm^{-3} and 5×10^{19} cm^{-3} [20].

Table 4 summarizes the comparison of the electrical characteristics of the c-Si solar cell with optimized BSF layer to that of the solar cell without a BSF layer. The efficiency in the solar cell with optimized BSF is considerably higher than that of the cell without BSF. This clearly demonstrates the importance of BSF in c-Si solar cells. V_{OC} of the cell with optimized BSF was 696.7 mV which is significantly higher than that of the cell without BSF where V_{OC} was 613.2 mV. Efficiency of the cell with optimized BSF and the cell without BSF were resulted in 18.02% and 15.11%, respectively.

Table 4. Comparison of the solar cell parameters with optimized BSF to that of the cell without BSF.

BSF	Voc (mV)	Jsc (mA/cm^2)	FF (%)	Eff (%)
Non-BSF	613.2	29.71	82.92	15.11
Optimized BSF	696.7	32.06	80.69	18.02

3.2. Determining the Optimal Firing Temperature

In addition to the optimization study of the BSF thickness and concentration using Afors-Het, BSF thickness dependence on the printed Al paste amount and the peak firing temperature was estimated using Equations (1) and (2) utilizing to the Al-Si phase diagram [17]. 12.6 wt% ratio of silicon in Al-Si alloy at eutectic temperature was used in calculations since it is mostly reported ratio in the literature [21-23]. Amount of Al was varied from 3 mg/cm^2 to 9 mg/cm^2 in the calculations of BSF thicknesses in order to determine the optimum peak firing temperature for each case.

Thickness of resulted BSF increases with either increasing the peak firing temperature or the amount of printed Al (Figure 5). In order to obtain the optimum BSF thickness of around 7 µm, the peak temperature should be adjusted by the amount of printed Al in consideration. For instance, temperature of up to 950ºC should be established if an amount of 3 mg/cm^2 printed Al was used to achieve BSF thickness of 7 µm, where 775ºC would be enough when the amount of Al is 8 mg/cm^2. Considering the average amount of printed Al is 6 or 7 mg/cm^2, a peak firing temperature of 825ºC and 800ºC need to be reached respectively, in order to form a 7 µm Al-BSF. Table 5 summarizes the calculated BSF thicknesses depending on the temperature and the amount printed Al paste.

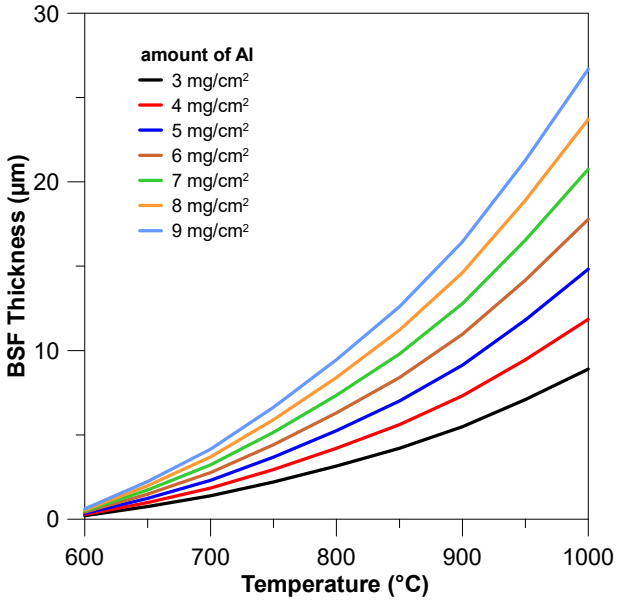

Figure 5. BSF thickness dependence to the peak firing temperature and the amount of Al.

Table 5. BSF thickness dependence on the peak firing temperature and the printed amount of Al paste.

		m_{Al} (mg/cm^2)							
		3	4	5	6	7	8	9	
T (°C)	600	0.205	0.273	0.342	0.410	0.478	0.547	0.615	BSF Thickness (µm)
	625	0.415	0.555	0.693	0.832	0.970	1.109	1.248	
	650	0.743	0.992	1.239	1.487	1.735	1.983	2.231	
	675	0.989	1.319	1.649	1.979	2.308	2.638	2.968	
	700	1.382	1.843	2.305	2.766	3.227	3.687	4.148	
	725	1.796	2.395	2.994	3.593	4.192	4.791	5.390	
	750	2.209	2.946	3.683	4.419	5.156	5.892	6.629	
	775	2.667	3.556	4.446	5.335	6.224	7.114	8.003	
	800	3.151	4.201	5.252	6.302	7.352	8.402	9.453	
	825	3.609	4.812	6.016	7.219	8.422	9.625	10.828	
	850	4.203	5.604	7.005	8.406	9.806	11.208	12.609	
	875	4.747	6.329	7.912	9.494	11.076	12.659	14.241	
	900	5.481	7.308	9.135	10.962	12.789	14.616	16.443	
	925	6.035	8.047	10.059	12.070	14.082	16.094	18.106	
	950	7.091	9.455	11.819	14.182	16.546	18.910	21.274	
	975	7.817	10.423	13.029	15.634	18.241	20.846	23.452	
	1000	8.893	11.857	14.822	17.786	20.750	23.715	26.679	

These optimization and results are supportive to realize the effect of BSF on the performance of c-Si solar cells. More importantly, these findings can be rewarding to understand the correlation between the printed Al paste and resulting BSF thickness which would be helpful for research of solar cells with thinner wafers.

4. CONCLUSIONS

In this article, the effects of the BSF layer on c-Si solar cells were investigated and optimized using Afors-Het simulation software. Photovoltaic parameters were determined depending on the BSF thickness of the c-Si solar cell. The maximum and close yield was obtained for the BSF thickness range of 6 µm to 8 µm. The optimum value of BSF doping concentration was in the order of 10^{19} cm^{-3}. The efficiency of c-Si solar cell without BSF (15.11%) could be improved with utilizing an optimum BSF up to 18.02%. Additionally, a special attention was given to the estimation of peak firing temperature depending on the printing amount of Al paste. It was concluded that the required peak firing temperature changes by the amount printed Al in order to form an optimal BSF. For instance, a peak firing temperature of 825°C need to be reached when the amount of printed Al is 6 mg/cm^2 to form a 7 µm Al-BSF. This study can be supportive to understand the importance of BSF structure for solar cells and to estimate the peak firing temperature depending on the amount of printed Al.

Research and Publication Ethics

Authors assure that this study was carried out by observing the international ethical rules of research and publication.

Ethics Committee Approval

This paper does not require any ethics committee permission or special permission.

Conflict of interest

Authors declared no conflict of interest.

Author's contributions

IK: investigation, methodology, simulation, data analysis, writing-initial draft. AU: supervision, conceptualization, methodology, investigation, data analysis, writing-revision and finalizing

REFERENCES

[1] M. M. Desa *et al.*, "Silicon back contact solar cell configuration: A pathway towards higher efficiency," *Renewable and Sustainable Energy Reviews,* vol. 60, pp. 1516-1532, 2016.

[2] S. Tobbeche and M. N. Kateb, "Simulation and Optimization of Silicon Solar Cell Back Surface Field," *Materials Science,* vol. 21, no. 4, pp. 491-496, 2015.

[3] A. Kaminski *et al.*, "Aluminium BSF in silicon solar cells," *Solar Energy Materials and Solar Cells,* vol. 72, no. 1-4, pp. 373-379, 2002.

[4] M. C. Raval and S. M. Reddy, "Industrial Silicon Solar Cells," in *Solar Cells*: IntechOpen, 2019.

[5] N. Balaji, M. C. Raval, and S. Saravanan, "Review on Metallization in Crystalline Silicon Solar Cells," in *Solar Cells*: IntechOpen, 2019.

[6] H. Yin, K. Tang, J. Zhang, W. Shan, X. Huang, and X. Shen, "Bifacial n-type silicon solar cells with selective front surface field and rear emitter," *Solar Energy Materials and Solar Cells,* vol. 208, p. 110345, 2020.

[7] R. Varache, C. Leendertz, M. Gueunier-Farret, J. Haschke, D. Muñoz, and L. Korte, "Investigation of selective junctions using a newly developed tunnel current model for solar cell applications," *Solar Energy Materials and Solar Cells,* vol. 141, pp. 14-23, 2015.

[8] M. Schmidt *et al.*, "Physical aspects of a-Si: H/c-Si hetero-junction solar cells," *Thin Solid Films,* vol. 515, no. 19, pp. 7475-7480, 2007.

[9] M. H. Vishkasougheh and B. Tunaboylu, "Simulation of high efficiency silicon solar cells with a hetero-junction microcrystalline intrinsic thin layer," *Energy conversion and management,* vol. 72, pp. 141-146, 2013.

[10] N. Dwivedi, S. Kumar, A. Bisht, K. Patel, and S. Sudhakar, "Simulation approach for optimization of device structure and thickness of HIT solar cells to achieve∼ 27% efficiency," *Solar energy,* vol. 88, pp. 31-41, 2013.

[11] T. Lauinger, J. Schmidt, A. G. Aberle, and R. Hezel, "Record low surface recombination velocities on 1 Ω cm p-silicon using remote plasma silicon nitride passivation," *Applied physics letters,* vol. 68, no. 9, pp. 1232-1234, 1996.

[12] J. G. Fossum, "Physical operation of back-surface-field silicon solar cells," *IEEE Transactions on Electron Devices,* vol. 24, no. 4, pp. 322-325, 1977.

[13] S. Riegel, S. Gloger, B. Raabe, and G. Hahn, "Comparison of the passivation quality of boron and aluminum BSF for wafers of varying thickness," in *24th European Photovoltaic Solar Energy Conference*, 2009, pp. 1596-1599.

[14] J. Szlufcik, S. Sivoththaman, J. Nlis, R. P. Mertens, and R. Van Overstraeten, "Low-cost industrial technologies of crystalline silicon solar cells," *Proceedings of the IEEE,* vol. 85, no. 5, pp. 711-730, 1997.

[15] L. J. Caballero, "Contact definition in industrial silicon solar cells," *Solar Energy,* pp. 375-398, 2010.

[16] F. Huster, "Aluminum-back surface field: bow investigation and elimination," in *20th European Photovoltaic Solar Energy*

Conference and Exhibition, Barcelona, pp. 635-638, 2005.

[17] J. Murray and A. McAlister, "The Al-Si (aluminum-silicon) system," *Bulletin of alloy phase diagrams,* vol. 5, no. 1, p. 74, 1984.

[18] M. B. Djurdjević, S. Manasijević, Z. Odanović, and N. Dolić, "Calculation of liquidus temperature for aluminum and magnesium alloys applying method of equivalency," *Advances in Materials Science and Engineering,* vol. 2013, 2013.

[19] I. Cesar *et al.*, "Industrial application of uncapped Al 2 O 3 and firing-through Al-BSF in open rear passivated solar cells," in *2011 37th IEEE Photovoltaic Specialists Conference*, pp. 001405-001410: IEEE, 2011.

[20] J. Eguren, J. Del Alamo, and A. Luque, "Optimisation of p+ doping level of n+-p-p+ bifacial bsf solar cells by ion implantation," *Electronics Letters,* vol. 16, no. 16, pp. 633-634, 1980.

[21] M. Barbes, M. Quintana, L. Verdeja, and R. Gonzalez, "Microstructures of a pressure die cast Al-8.5% Si-3.5% Cu alloy," *Kovove Mater,* vol. 55, pp. 89-96, 2017.

[22] A. Sharma and J. P. Jung, "Possibility of Al-Si Brazing Alloys for Industrial Microjoining Applications," *Journal of the Microelectronics and Packaging Society,* vol. 24, no. 3, pp. 35-40, 2017.

[23] M. Haghshenas and J. Jamali, "Assessment of circumferential cracks in hypereutectic Al-Si clutch housings," *Case Studies in Engineering Failure Analysis,* vol. 8, 12/01 2016.